AIAA-89-1973
A Numerical Study of Shock Wave Refractions at a Gas Interface

P. Colella
University of California
Berkeley, CA
L. Henderson
University of Sydney
New South Wales, AUSTRALIA
E. Puckett
Lawrence Livermore National Laboratory
Livermore, CA

AIAA 9th Computational Fluid Dynamics Conference
Buffalo, New York / June 13–15, 1989

A NUMERICAL STUDY OF SHOCK WAVE REFRACTION AT A GAS INTERFACE*

Phillip Colella**
University of California at Berkeley
Berkeley, CA 74720

Leroy F. Henderson†
University of Sydney
New South Wales 2006, Australia

Elbridge Gerry Puckett‡
Lawrence Livermore National Laboratory
Livermore, CA 94550

Abstract

This paper describes the numerical simulation of a shock wave refracting at a gas interface. In this work we duplicate shock tube experiments performed by Abd-el-Fattah and Henderson using a multifluid, adaptive mesh refinement algorithm. We report on the results of four of these calculations and compare them to the shock tube experiments. The goal of this paper is to validate the numerical method by demonstrating that the numerical results are in excellent agreement with the shock tube experiments. Future work will be concerned with using our numerical method to explore the phenomenon of shock wave refraction and with examining the discrepancy between existing theory and experiment.

The Problem

In this work we consider a planar shock wave striking a planar gas interface at angle of incidence $0° < \omega_i < 90°$. This is a predominantly two dimensional, inviscid phenomenon which we model using the two dimensional Euler equations with the incident shock wave and gas interface being represented by straight lines.

A diagram of the experimental setup is shown in figure 1. The shock wave travels from right to left in the incident gas striking the interface from the right. This causes a shock wave to be transmitted into the transmission gas and a reflected wave to travel back into the incident gas. This reflected wave can either be a shock, an expansion, or a band of compression waves. Depending on the strength of the incident shock, the angle of incidence, and the density and sound speeds of the two gases these three waves may appear in any one of several distinct configurations. In the simplest case the reflected wave is a shock and all three shocks meet at a single point on the interface and travel at the same speed along the interface. This is known as regular refraction.

When the sound speed of the incident gas is less than that of the transmission gas the refraction is called *slow-fast*. In this case the transmitted shock can break away from the point of intersection and move ahead of the other two waves, forming what is known as a precursor shock. The incident shock can also form a Mach stem, similar to the well know phenomenon of Mach reflection at a ramp. When the sound speed of the incident gas is greater than that of the transmission gas the refraction is called *fast-slow*. In this case the transmitted shock will lean back toward the interface. Under these circumstances one can observe roll up of the gas interface and acoustic waves transmitted back into the incident gas.

For the purposes of modeling this phenomenon on a computer we assume the two gases are ideal and that each gas satisfies a γ law equation of state,

$$p = A\,\rho^{\gamma}.$$

Here p is the pressure, ρ the density, γ the ratio of specific heats, and A a constant which depends on the entropy but is independent of p and ρ. Note

* Work performed under the auspices of the U.S. Department of Energy at the Lawrence Livermore National Laboratory under contract number W-7405-ENG-48 and partially supported by the Applied Mathematical Sciences subprogram of the Office of Energy Research under contract number W-7405-Eng-48 and the defense Nuclear Agency under IACRO 88-873.

** Associate Professor, Mechanical Engineering, Member AIAA

† Professor, Mechanical Engineering

‡ Postdoctoral Fellow, Applied Mathematics Group, Member AIAA

that γ is a constant for each fluid but different fluids will have different γ.

Given the assumptions stated above the problem may be shown to depend on the following four parameters: the angle of incidence ω_i, the ratio of molecular weights for the two gases μ_i/μ_t, the ratio of the γ for the two gases γ_i/γ_t, and the incident shock strength $\xi_i = p_1/p_0$ where p_0 (*respectively* p_1) is the pressure on the upstream (*respectively* downstream) side of the shock. Theories have been developed based on these assumptions which are generally in good agreement with experiment. For example, early work on the theory of regular refraction was done by Taub[1] and Polachek & Seeger.[2] Later, Henderson[3] extended this work to irregular refractions. More recently, Henderson[4,5] has generalized the definition of shock wave impedance given by Polachek & Seeger for the refraction of normal shocks.

Experiments with shock waves refracting in gases have been done by Jahn,[6] Abd-el-Fattah, Henderson & Lozzi,[7] and Abd-el-Fattah & Henderson.[8,9] Our work is based on the experiments reported on in these last two papers. More recently, Reichenbach[10] has done experiments with shocks refracting at thermal layers and Haas & Sturtevant[11] have studied refraction by gaseous cylindrical and spherical inhomogeneities. Earlier, Dewey[12] reported on precursor shocks from large scale explosions in the atmosphere. Some multiphase experiments have also been done: Sommerfeld[13] has studied shocks refracting from pure air into air containing dust particles while Gvozdeava *et al.*[14] have experimented with shocks passing from air into a variety of foam plastics.

Some recent numerical work on shock wave refractions include Picone *et al.*[15] who studied studied the Haas & Sturtevant experiments at Air/He and Air/Freon cylindrical and spherical interfaces. Fry & Book[16] have considered refraction at heated layers and Glowacki *et al.*[17] have studied refraction at high speed sound layers. Sugimura, Tokita & Fujiwara[18] have examined refraction in a liquid-bubble system.

Description of the Shock Tube Experiments

In this paper we duplicate four of the shock tube experiments from Abd-el-Fattah and Henderson.[8,9] Two of the experiments are in the slow-fast regime (CO_2/CH_4) and the other two are fast-slow (Air/SF_6). The experiments were performed in a conventional shock tube with air as a driver. The layout of the apparatus for the case when the incident gas is CO_2 and the transmission gas is CH_4 is shown in figure 2. The separation between the two gases was maintained by a thin polymer membrane (labeled 'm' in figure 2). The thickness of this membrane was measured to be between 5.5 and 6.5×10^{-6} cm. This is on the order of only 10 molecules thick. Much effort was made toward making the membrane as thin as possible in order to minimize the effects of the mass of the membrane on the refracting shock wave system. However the thiness of the membrane resulted in some mixing of the two gases at the interface. The amount of leakage was measured using a gas analyzer (labeled 'GA' in figure 2). Both the effects of the membrane inertia and the gas mixing have been carefully studied and reported on by Abd-el-Fattah, Henderson & Lozzi.[7] For further details of the experimental apparatus and experimental results the reader is referred to Abd-el-Fattah, Henderson, & Lozzi[7] and Abd-el-Fattah and Henderson.[8,9]

In the numerical results described below the two gases were assumed to be uncontaminated and separated by a massless membrane. We also performed calculations in which we included a membrane with the same mass as that used in the laboratory and took into account the measured amount of contamination of the gases during our computation of the equation of state. The results of these latter experiments differed little from those described below. The greatest change appeared to be in the angle that the transmitted shock made with the interface (in the slow-fast case) but this angle is difficult to measure accurately. We will not discuss the effects of the membrane or gas contamination further and simply assume idealized conditions for our numerical experiments.

The Numerical Method

We solve the Euler equations for two dimensional, compressible fluid flow in conservation form

$$\mathbf{U}_t + \nabla \cdot \mathbf{F}(\mathbf{U}) = 0. \qquad (1)$$

Here

$$\mathbf{U} = (\rho, \rho u, \rho v, \rho E)^T$$

where (u,v) is the velocity, E the total energy per unit mass, and $\mathbf{F} = (F,G)^T$ with

$$F = (\rho u, \rho u^2 + p, \rho u v, \rho u E + u p)^T,$$

$$G = (\rho v, \rho u v, \rho v^2 + p, \rho v E + v p)^T.$$

We solve these equations on a rectangular mesh with grid spacing Δx and Δy. We use absorbing

boundary conditions on the right hand wall of the computational domain and reflecting boundary conditions on the other three walls.

The following four features of our numerical method are important in the accurate computation of the shock refraction problem.

1) A second order Godunov method for solving the fluid flow equations

2) An local, adaptive gridding strategy

3) A volume of fluid strategy for tracking the fluid interface based on tracking partial volumes of fluid components on a subgrid scale

4) An algorithm for accurately modeling the disparate thermodynamic properties of the two gases on a subgrid scale.

Currently we use an operator split version of the numerical method. In other words, we solve a succession of one dimensional problems at each time step, alternating the x and y sweeps at every other time step. Effective unsplit techniques are available for solving equations (1) but operator splitting is necessitated by the interface tracking algorithm we use. We are currently developing an improved interface algorithm that will remove this restriction and we will report on it in a future work.

The Solution of the Euler equations

We use a second order Godunov method to solve the two dimensional compressible Euler equations. Since these methods have been widely discussed in the literature we refrain from going into detail here. Instead we refer the interested reader to van Leer,[19] Colella & Woodward,[20] and Colella & Glaz.[21] It should be remarked that in this work we use a piecewise linear approximation to the quantities in each grid cell rather than a piecewise parabolic approximation as discussed in Colella & Woodward.[20]

Adaptive Mesh Refinement

In order to concentrate most of the computational work in regions of physical interest we employ a local adaptive gridding strategy called Adaptive Mesh Refinement (AMR).[22,23,24,25,26] The basic idea behind AMR is to estimate the local truncation error at each cell center and tag those cells at which the error is unacceptably large. One then finds a collection of rectangles, all of which are contained in the original grid, in such a way that each of the tagged cells is contained in one of these rectangles and such that a minimum number of untagged cells are also included. The optimum set of rectangles is also chosen with regard to minimizing a cost function. So, for example, one large rectangle may be chosen instead of two smaller rectangles with fewer untagged grid points because it leads to more optimal vector lengths on the Cray. This cost function also takes into account the overhead associated with setting up the boundary conditions for each fine grid.

Each of these new rectangles is then subdivided into smaller cells $1/k$ th the size of the original coarse cell (generally $k = 2$ or 4) and the values of the state variables are assigned to each of the new cells in such a way as to conserve all of the appropriate quantities. The equations of motion are then solved on the finer mesh with boundary values obtained from adjacent grids of the same level of refinement or interpolated from the coarser mesh. Note that in order for the CFL condition to be satisfied one must take k times as many time steps on the finer grid, each $1/k$ th the size of the coarse grid time step. The value of the state variables in a coarse grid cell which contains fine grid cells is set to the average of the values in the fine grid cells. In order to guarantee conservation at grid boundaries care is taken so that if the boundary of a fine grid abuts a coarse grid (and not another fine grid), then the flux across each coarse cell wall is equal to the sum of the fluxes out of each fine cell wall which abuts the coarse cell. We then recursively extend this procedure to obtain multiple levels of refinement.

Figure 3 contains the contour plot of log p with the fine grid boundaries overlaid on top. This plot is from the computation described in figure 8 and was run with one level of refinement and a refinement factor of 4. Note that fine grids are allowed to overlap since this may lead to better vector lengths and hence better performance. For further details regarding our implementation of the AMR algorithm the reader is referred to Berger & Colella.[26]

Tracking the Gas Interface

We employ a partial volumes based approach to the problem of tracking the gas interface. Figure 4 depicts a portion of the interface and its intersection with several grid cells. At the start of the computation we calculate for each cell the ratio f_{ij} of volume occupied by the dark fluid to the total volume of the cell. So $0 \le f_{ij} \le 1$ for all cells with

$f_{ij} = 0$ if the cell contains all light fluid and $f_{ij} = 1$ if the cell contains all dark fluid. At each time step the interface is advanced in time as follows:

1) Given the partial volumes f_{ij} we create an approximation to the interface in each multifluid cell ($0 < f_{ij} < 1$), such that this approximate interface divides the cell into the correct ratio of fluid volumes.

2) For the x-sweep we divide the cell by a vertical line into two rectangles with areas $|u|\Delta t\,\Delta y$ and $(\Delta x - |u|\Delta t)\Delta y$. We then move that portion of the dark fluid which lies inside the rectangle on the right (if $u > 0$ and on the left if $u < 0$) into the adjacent cell (right if $u > 0$ and left if $u < 0$). A cartoon depicting an example of this procedure when $u > 0$ is shown in figure 4. An identical procedure is performed for the y-sweep with u replaced by v, Δy replaced by Δx, etc.

It remains for us to specify how one recreates the interface given the partial volumes f_{ij}. Here we employ the SLIC (Simple Line Interface Calculation) algorithm created by Noh and Woodward.[27] In determining the interface in the i,jth cell for an x-sweep SLIC considers only the ratio f_{ij} in that cell and the presence or absence of light and dark fluids in the two adjoining (in the x-direction) cells. Figure 5 depicts how the interface is drawn in three of the five possible cases. Reversing the roles of light and dark fluid yields the other two cases. (Case 5b) remains the same when the dark and light fluids are reversed.) Figure 6 contains an example of how the SLIC algorithm would reconstruct the interface in figure 4. The interface is reconstructed in an analogous manner for a sweep in the y-direction.

It should be emphasized that the only feature of the flow which we are tracking is the actual gas interface. All of the shocks and other discontinuities in the flow are *captured* by the underlying solution of the equations of gas dynamics.

Subgrid Modeling of the Multifluid Components

We employ a new innovation for modeling the thermodynamic properties of distinct fluid components which occupy the same grid cell. The principle goal of this algorithm is to ensure that fluid components of different densities will undergo the correct relative compressions or expansions when the cell they occupy is subjected to pressure forces. This algorithm is based on the assumption that the various fluid components in each cell are in pressure equilibrium with one another and that each cell has a single velocity. From a physical point of view the assumption of pressure equilibrium is not unreasonable since pressure is continuous across a contact discontinuity. The requirement that the cell have a single velocity is not appropriate in more than one dimension since slip will be generated at a fluid interface. Thus we track the jump in thermodynamic variables across the interface, while capturing the jump in tangential velocity using the underlying conservative finite difference method. This algorithm is applicable to any number of fluid components. We refer the reader to Colella, Glaz & Ferguson[28] for a detailed description of this algorithm.

Results

We report on the results of four calculations, two slow-fast and two fast-slow. Each of figures 7-10 contain a schlieren photo of a shock tube experiment and two contour plots from the corresponding computation. We show the contours for a variety of different quantities in order to give the reader an idea of how different quantities reproduce the phenomena being studied. In all of the photos and contour plots there is a line running diagonally from upper left to lower right. This line represents the initial gas interface before being struck by the shock. In the schlieren photos this line is part of a wire frame which holds the membrane in place. In the contour plots it is simply a line drawn for easy reference and is not a contour of the quantity being plotted.

Slow-Fast

Figures 7 and 8 contain the results of the two slow-fast experiments. In both experiments the gas interface is CO_2/CH_4 and the initial shock strength is $\xi_i = 1.89$. The only difference between the two experiments is that the angle of incidence ω_i has been changed from 50.5° to 62°. Both refractions are irregular with a precursor shock in the CH_4. There is a shock wave refracting back from this precursor into the incident gas which meets and disturbs the incident shock close to the interface. In both cases there is also a reflected shock or band of compression waves which meets the incident shock at the bottom of its undisturbed portion and points back into the incident gas.

In the first refraction the disturbed portion of the incident shock consists of one short segment or 'stem' which runs directly from the undisturbed portion to the interface. All four shocks and a slip line meet at the base of the undisturbed part of the incident shock, with the slip line running parallel to

the disturbed interface. In the second refraction however the disturbed portion of the incident shock has two distinct sections. The intersection of these two sections and the intersection of the upper section with the undisturbed incident shock are triple points at which three shocks and a slip line meet. Abd-el-Fattah & Henderson[9] refer to this configuration as a 'Twin von Neumann refraction'.

Most of these features appear clearly in the contour plots accompanying the photographs. All of the shocks appear as dark lines where many contours have been drawn one on top of the other. The reflected waves appear as a sharp jump in both pressure and density followed by bands of contours. The contour plot of the pressure (see also figure 3) allows one to easily examine the pressure field, something which is very difficult to achieve with experimental apparatus. By marking the contours with their values or plotting the contours in color one can easily distinguish between compressions and expansions.

The most difficult features to resolve with contour plots are the slip lines. It should be emphasized that this is not a difficulty with the computation of the flow field but rather a difficulty with flow visualization via the contour plots. (Of course one does not expect slip lines to appear in the pressure contours.) The slip lines are somewhat apparent in a bending of the density contours in figures 7b) and 8b). These slip lines will appear quite clearly in a contour plot of the vorticity, but because the vorticity is obtained by differencing the values of the velocity at grid points there are large numerical errors near some of the shocks. We have found that the best visualization of the slip line discontinuities is obtained with color contours.

Fast-Slow

In figures 9 and 10 we have reproduced schlieren photographs of two fast-slow refractions and contour plots from the corresponding computations. In both cases the refraction is from Air into SF_6. The incident shock in figure 9 is very weak with $\xi_i = 1.1$ while in figure 10 we have a strong incident shock with $\xi_i = 4$. The angle of incidence is similar in both cases: $\omega_i = 79$ in figure 9 and $\omega_i = 73.5$ in figure 10.

A remark should be made here regarding contour plots. Each plot has thirty contours which represent thirty values of the variable in question, taken in equal increments between its minimum and maximum values. Thus, if most of the variation in a given quantity occurs in one region, say at a very large jump, then all of the contour lines will be absorbed by this jump and little will be revealed of the remaining (often more interesting) variation of that quantity. Color contour plots will reveal this latter variation as slightly different shades of the same color and hence are often more satisfying than the contour line plots. This problem is especially pervasive in the Air/SF_6 studies where the jump across the gas interface in a given quantity is often more than ten times the size of the variation found in the other wave patterns. Thus, in order to focus on these patterns we sometimes found it necessary ignore the variation across the disturbed interface. For example, figure 9b) is a contour plot only of the density variation in the incident gas. Similarly, in figure 10c) the contours only represent the variation in the upper 20% of values for the total energy. (The pair of vertical lines in the middle of this plot are due to spurious numerical 'start up' error. This is a sort of ghost signal from the initial incident shock. With a little effort this signal could be damped. However this would be a primarily cosmetic effort since the error is mostly unsightly and not terribly damaging. For a more detailed discussion of this type of numerical error see Noh.[29])

In the fast-slow refractions it is immediately apparent that the transmitted shock trails behind the incident shock. This is because of the lower sound speed in SF_6. In both cases the transmitted shock reflects off the bottom plate, bounces back, and strikes the interface. In fact, in figure 9 this happens at least twice. Another important feature of the refraction in figure 9 is an expansion wave which begins where the incident shock meets the interface and reflects back into the incident gas. This wave is barely visible in the photograph whereas the contour plots reveal the structure of this wave quite nicely.

The photograph in figure 10a) exhibits several interesting features. There are very pronounced acoustic waves radiating out from the region where the transmitted wave has reflected back and struck the interface. Also note the entropy wave which starts from the point where the outermost acoustic wave touches the incident shock and runs at an angle back toward the source of the acoustic signal. There is also the slightest hint of an expansion which begins at the intersection of the incident shock with the interface. These features appear fairly clearly in the contour plot of total energy shown in figure 10c).

Another interesting feature of this refraction is the roll up of the fluid interface. This is virtually invisible in the schlieren photographs yet readily apparent in the contour plot of density. On the

basis of our work here we conjecture that the acoustic signals observed in figures 10a) and 10c) are caused by the interaction of a vortex with the reflection of the transmitted shock which has bounced off the bottom plate and struck the disturbed interface as it is rolling up.

Conclusions

It is apparent that the numerical results agree quite well with the large scale features observed in the shock tube experiments. The only noticeable discrepancy between the computations and shock tube experiments is the movement of the disturbed gas interface at the bottom wall. However this is as it should be since our numerical method is solving the (inviscid) Euler equations and hence, not accounting for viscous effects near the wall. All inviscid phenomenon, in particular all of the shock wave interactions with each other and with the gas interface, have been reproduced with quite satisfying accuracy.

We have also made several sequences of runs in which the two gases and the incident shock strength were fixed and the angle of incidence ω_i was varied. We measured the angles which various waves make with each other and noted the angles at which the shock wave system transitions from one configuration to another. Our preliminary results indicate that these measurements also agree quite well with experiment. We plan to publish this data in a future paper.

Acknowledgements

The photographs in figures 7a) & 8a) and figures 9a) & 10a) are from Abd-el-Fattah & Henderson[9] and Abd-el-Fattah & Henderson[8] respectively and are reproduced with permission of the authors.

References

1. A. H. Taub, "Refraction of plane shock waves," *Phys. Rev*, vol. 72, pp. 51-60, 1947.
2. H. Polachek and R. J. Seeger , "On shock wave phenomenon: refraction of shock waves at a gaseous interface," *Phys. Rev.*, vol. 84 , pp. 922-929, 1951.
3. L. F. Henderson, "The refraction of a plane shock wave at a gas interface," *J. Fluid Mech.*, vol. 26, pp. 607-637, 1966.
4. L. F. Henderson, "On shock impedance," *J. Fluid Mech.*, vol. 40, pp. 719-735, 1970.
5. L. F. Henderson, "On the refraction of shock waves," *J. Fluid Mech.*, vol. 198, pp. 365-386, 1989.
6. R. G. Jahn, "The refraction of shock waves at a gaseous interface," *J. Fluid Mech.*, vol. 1, pp. 457-489, 1956.
7. A. M. Abd-el-Fattah, L. F. Henderson, and A. Lozzi, "Precursor shock waves at a slow-fast gas interface," *J. Fluid Mech.*, vol. 76, pp. 157-176, 1976.
8. A. M. Abd-el-Fattah and L. F. Henderson, "Shock waves at a fast-slow gas interface," *J. Fluid Mech.*, vol. 86, pp. 15-32, 1978.
9. A. M. Abd-el-Fattah and L. F. Henderson, "Shock waves at a slow-fast gas interface," *J. Fluid Mech.*, vol. 89, pp. 79-95, 1978.
10. H. Reichenbach, "Roughness and heated layer effects on shock wave propagation and reflection-experimental results," E-Mach Inst. Rep. E24/85, Frieberg: Fraunhofer-Gesellschaft, 1985.
11. J. F. Haas and B. Sturtevant, "Interaction with weak shock waves with cylindrical and sphereical gas inhomogeneities," *J. Fluid Mech.*, vol. 181, pp. 41-76, 1987.
12. J. M. Dewey, "Precursor shocks produced by a large yield chemical explosion," *Nature*, vol. 205, p. 1306, 1965.
13. M. Sommerfeld, "The unsteadiness of shock waves propogating through gas-particle mixtures," *Experiments in Fluids*, vol. 3, pp. 197-206, 1985.
14. L. G. Gvozdeava, X. Faresov, M. Yu, J. Brossard, and N. Charpentier, "Normal shock wave reflexion on porous compressible material," *Prog. Astron. Aeron.*, vol. 106, pp. 155-165, 1986.
15. J. M. Picone, J. P. Boris, E. S. Oran, and R. Ahearne, "Rotational motion generated by shock propagation through a non-uniform gas," in *Proc. 15th Intl. Symp. on Shock Waves and Shock Tubes*, ed. R. Hanson, pp. 523-529, Stanford University Press, 1986.
16. M. A. Fry and D. L. Book, "Shock dynamics in heated layers," in *Proc. 15th Intl. Symp. on Shock Waves and Shock Tubes*, ed. R. Hanson, pp. 523-529, Stanford University Press, 1986.
17. W. J. Glowacki, A. L. Kuhl, H. M. Glaz, and R. E. Ferguson, "Shock Wave Interaction with High Sound Speed Layers," in *Proc. 15th Intl. Symp. on Shock Waves and Shock*

Tubes, ed. D. Bershader & R. Hanson, pp. 523-529, Stanford University Press, 1986.

18. T. Sugimura, K. Tokita, and T. Fujiwara, "Nonsteady shock wave propagating in a bubble-liquid system," *Prog. Astron. Aeron.*, vol. 94, pp. 320-331, 1984.
19. B. van Leer , "Towards the Ultimate Conservative Differences Scheme, A Second Order Sequel to Godunov's Methods," *J. Comp. Phys.*, vol. 32, pp. 101-136, 1979.
20. P. Colella and P. Woodward, "The Piecewise Parabolic Method (PPM) for Gas Dynamical Simulations," *J. Comp. Phys.*, vol. 54, pp. 174-201, 1984.
21. P. Colella and H. M. Glaz, "Efficient Solution Algorithms for the Riemann Problem for Real Gases," *J. Comp. Phys.*, vol. 59, no. 2, pp. 264-289, 1985.
22. M. J. Berger and J. Oliger, "Adaptive mesh refinement for hyperbolic partial differential equations," *J. Comp. Phys*, vol. 53, pp. 482-512, 1984.
23. M. J. Berger and A. Jameson, "Automatic Adaptive Grid Refinement for the Euler Equations," *AIAA J.*, vol. 23, pp. 561-568, 1985.
24. M. J. Berger, "Data Structures for adaptive grid generation," *SIAM J. Sci. Stat. Comp.*, vol. 7, pp. 904-916, 1986.
25. M. J. Berger, "On Conservation at Grid Interfaces," *SIAM J. Num. Anal.*, 1987.
26. P. Colella and M. J. Berger, "Local Adaptive Mesh Refinement for Shock Hydrodynamics," *UCRL preprint #97196*, 1987.
27. W. F. Noh and P. Woodward, "SLIC (Simple Line Interface Calculation)," UCRL-77651, Lawrence Livermore Laboratory, 1976.
28. P. Colella, H. M. Glaz, and R. E. Ferguson, "Multifluid Algorithms for Eulerian Finite Difference Methods," *manuscript*, 1989.
29. W. F. Noh, "Numerical methods in hydrodynamic calculations," UCRL-77651, Lawrence Livermore Laboratory, 1976.

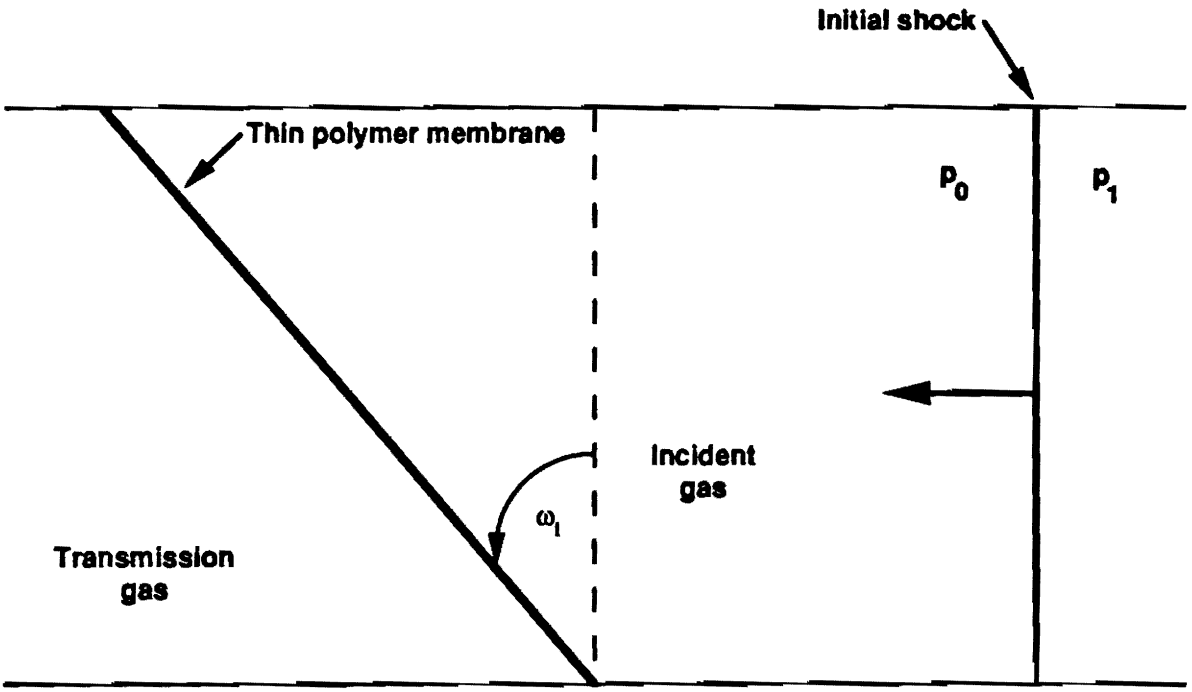

Figure 1. The problem

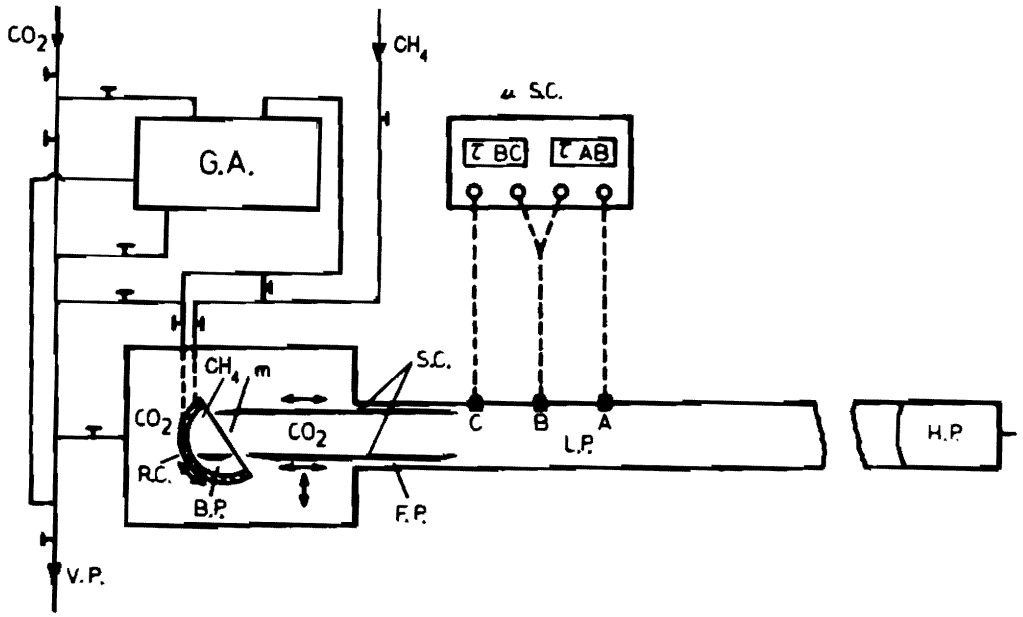

Figure 2. Layout of apparatus. G.A. thermal conductivity gas analyser; μ S.C. micro-second counter; S.C. shock cutter; L.P. low pressure driver section, CO_2 ; H.P. high pressure driving section with air as driver gas; V.P. vacuum pump; B.P. back plate; F.P. front plate.

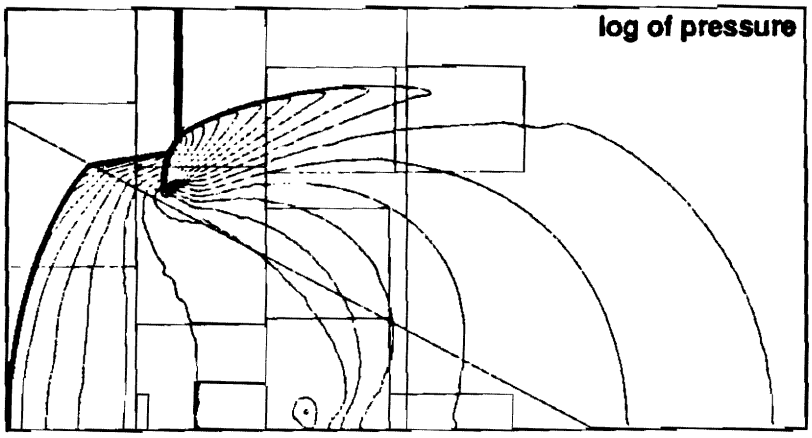

Figure 3. The boundaries of the fine grids have been superimposed over the contour plot of the log of the pressure. The case shown has one level of refinement and corresponds to figure 8.

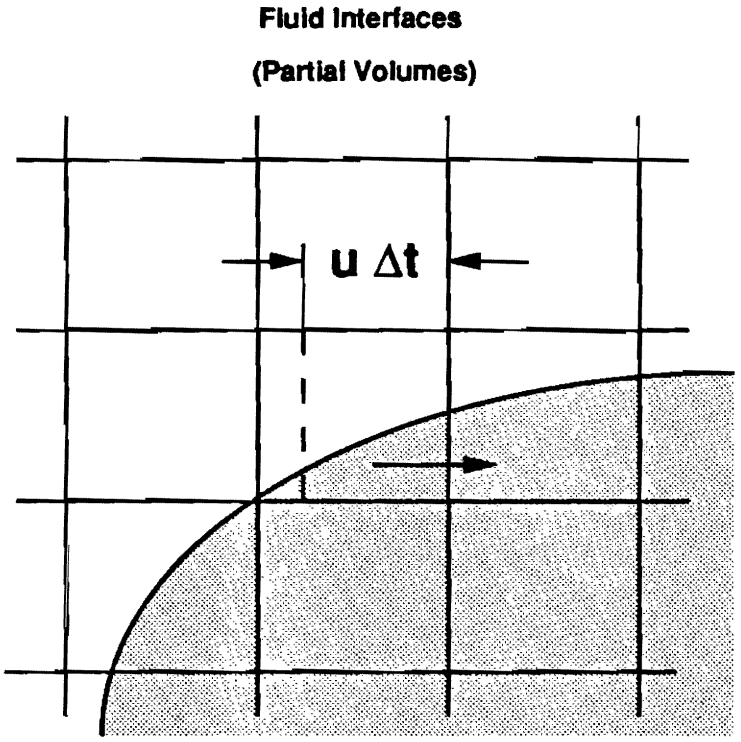

Figure 4. The fraction of dark fluid to the right of the dotted line is advected into the neighboring cell on the right. In this example u is positive.

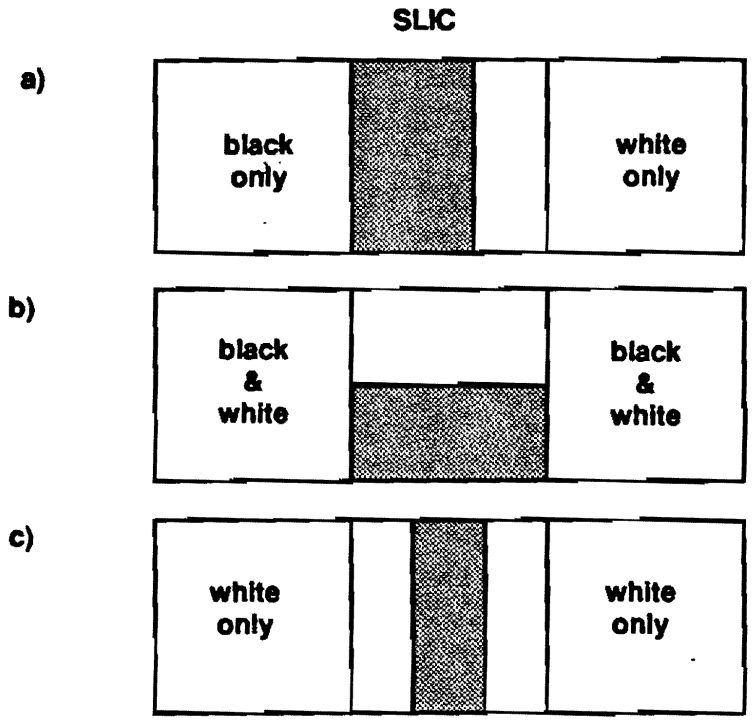

Figure 5. Given the states in the adjacent cells this is how SLIC will draw the interface for a pass in the x-direction. There are two other cases obtained by interchanging black and white in a) and c).

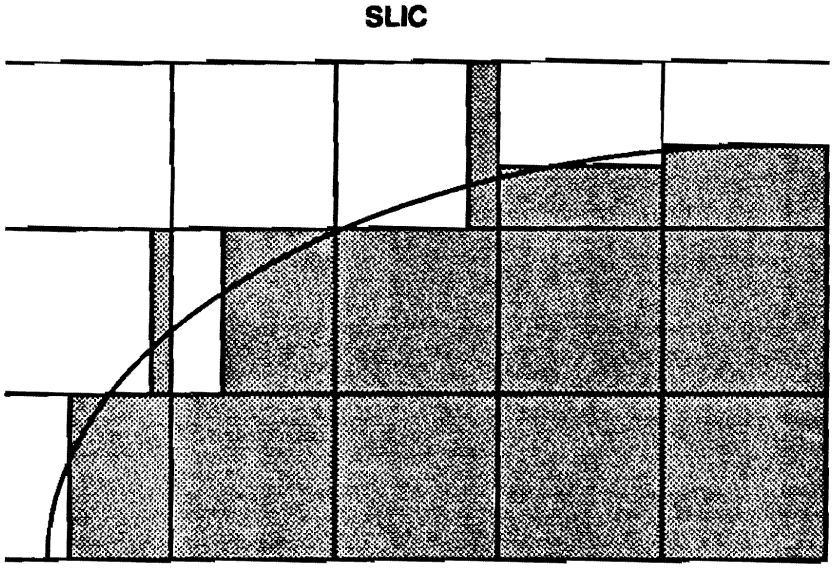

Figure 6. This is how SLIC would recreate the interface in figure 4 for a sweep in the x-direction.

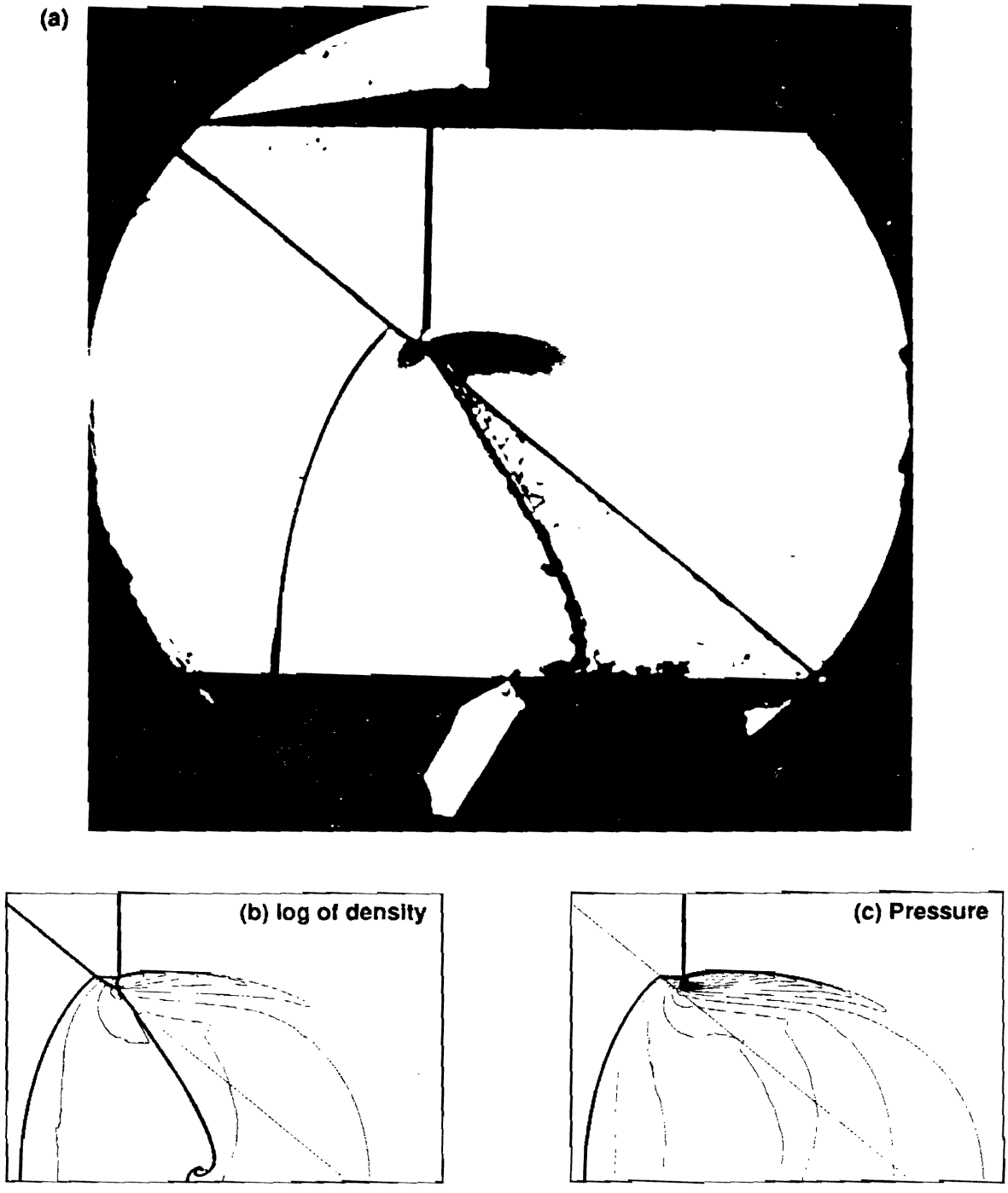

Figure 7. Free precursor irregular refraction at a CO_2/CH_4 (slow-fast) interface with incident shock strength $\xi_1 = 1.89$ and angle of incidence $\omega_1 = 50.5°$.

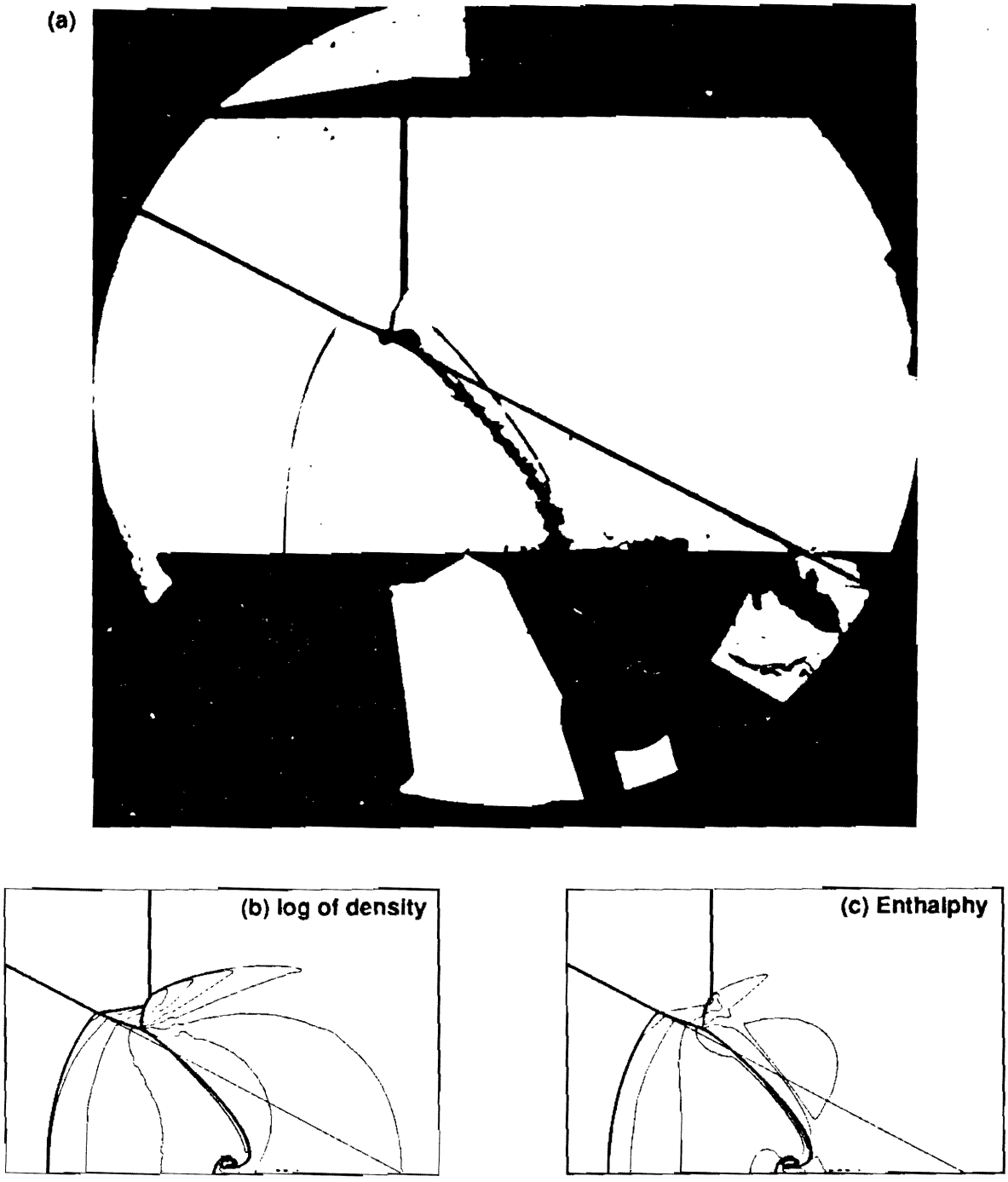

Figure 8. Twin von Neumann irregular refraction at a CO_2/CH_4 (slow-fast) interface with incident shock strength $\xi_i = 1.89$ and angle of incidence $\omega_i = 62°$.

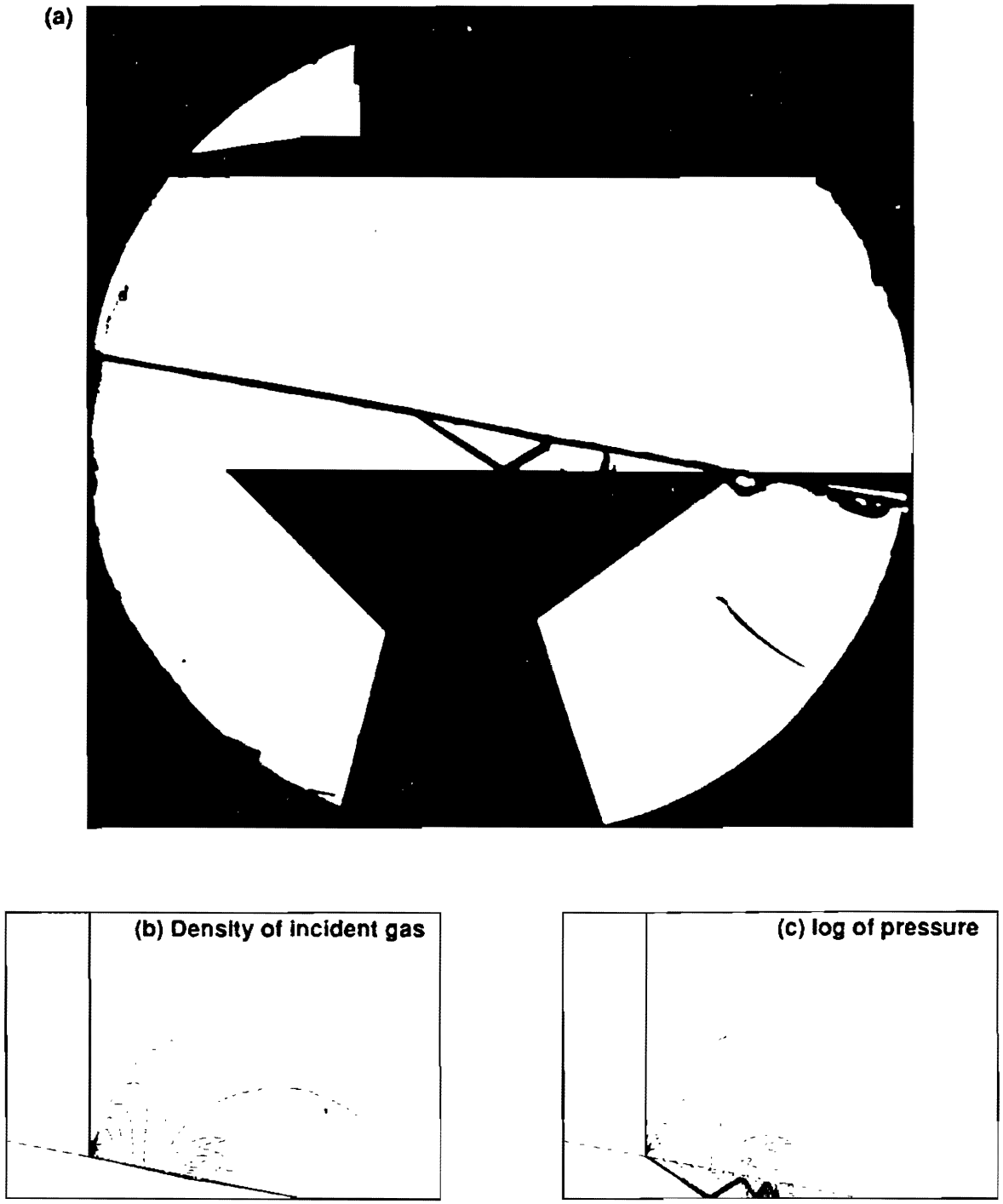

Figure 9. Irregular refraction at a Air/SF_6 (fast-slow) interface with incident shock strength $\xi_i = 1.1$ and angle of incidence $\omega_i = 79°$.

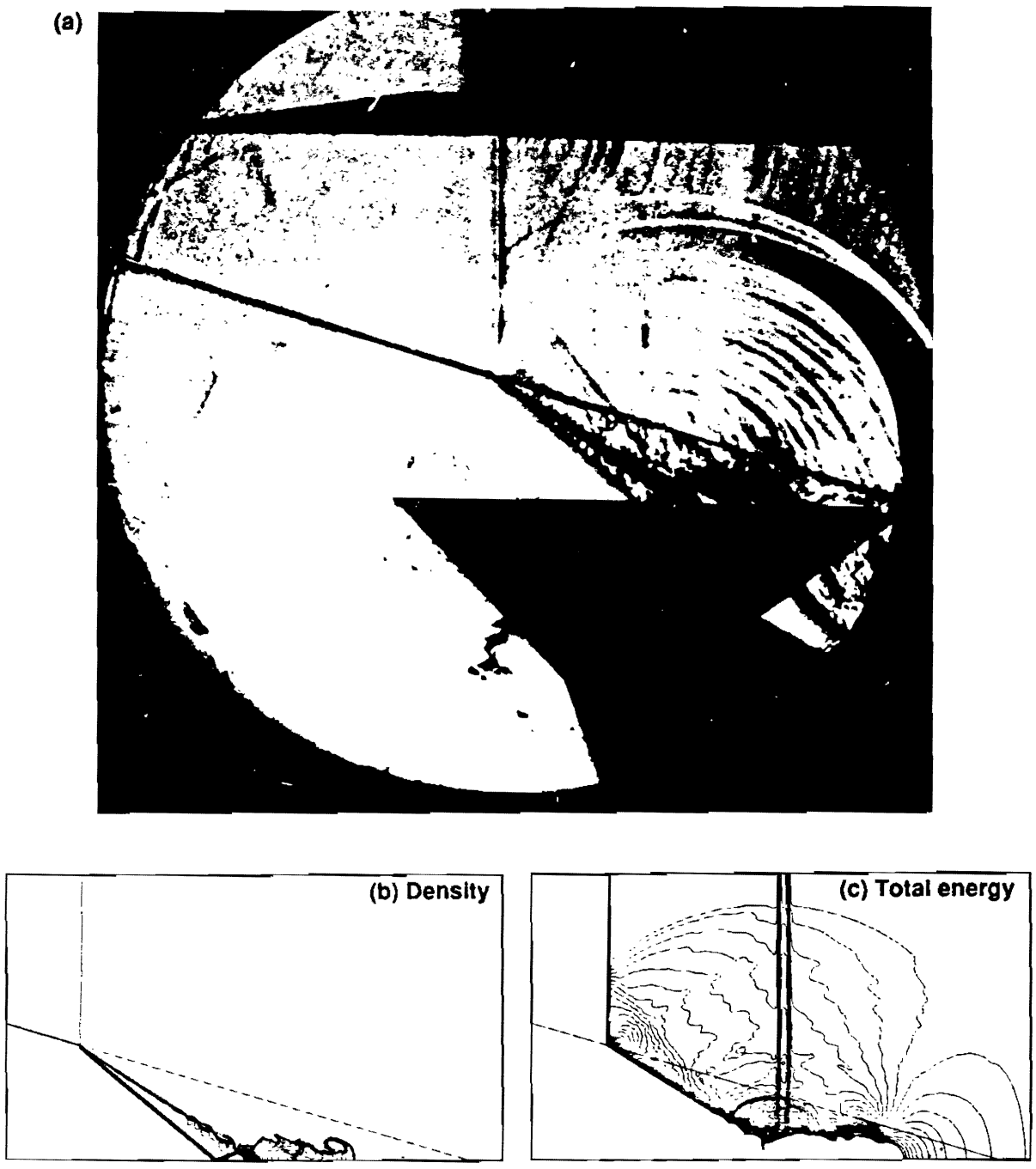

Figure 10. Irregular refraction at a Air/SF_6 (fast-slow) interface with incident shock strength $\xi_1 = 4.0$ and angle of incidence $\omega_1 = 73.5°$.